Magnetic phase transition in $MnCr_{2-2x}In_{2x}S_4$ crystals

1999 J. Phys.: Condens. Matter 11 7907

(http://iopscience.iop.org/0953-8984/11/40/315)

J. Phys.: Condens. Matter **11** (1999) 7907–7920. Printed in the UK PII: S0953-8984(99)00691-8

Magnetic phase transition in $MnCr_{2-2x}In_{2x}S_4$ crystals

V Tsurkan†‡§, M Baran†, A Szewczyk†, R Szymczak† and H Szymczak†

† Institute of Physics, Polish Academy of Sciences, Al Lotnikow 32/46, 02-668 Warsaw, Poland
‡ Institute of Applied Physics, Academy of Sciences of Moldova, Academiei str. 5, Kishinev, MD 2028, Republic of Moldova

E-mail: vtsurkan@phys.asm.md

Received 5 January 1999

Abstract. The influence of In for Cr substitution on the para- to ferrimagnetic phase transition has been investigated for $MnCr_{2-2x}In_{2x}S_4$ spinel crystals by means of DC magnetization measurements. The critical exponents β and γ calculated from the high field extrapolation of the modified Arrott plots were found to be unaltered with substitution and close to 3D Heisenberg ones. A considerable expansion of the temperature range of the upward curvature of the inverse initial susceptibility of the samples with disorder increase has been found. Non-monotonic temperature dependences of Kouvel–Fisher effective susceptibility exponent γ^* for disordered samples and the increase of the γ^* value with the In concentration growth were also observed.

1. Introduction

Ternary magnetic spinel semiconductor $MnCr_4S_4$ exhibits non-monotonic temperature dependence of the magnetization due to antiparallel alignment of the spins of A-site Mn and B-site Cr ions [1]. Magnetic dilution of the Cr sublattice with In was found to reduce the value of the magnetic moment [2]. Recently, re-entrant spin-glass and spin-glass-like behaviour of magnetization at low temperatures in $MnCr_{2-2x}In_{2x}S_4$ crystals have been observed [3]. These frustrated states were shown to appear due to fluctuation of the competing exchange interactions caused by disorder induced with In substitution.

The influence of disorder on the low temperature transition-like phenomena for ternary magnetic semiconductor compounds with spinel structure has been widely investigated (see, for example, [4]). Little information, however, is available about the disorder effect on the high temperature transition from ferro- (ferri-) to paramagnetic state. Not long ago, the data for a number of semi-disordered mixed spinel compounds have appeared, and large deviations from the Heisenberg values of the critical exponents have been reported [5].

In the $MnCr_{2-2x}In_{2x}S_4$ system a complete range of solid solutions exists and thus the disorder degree of the crystals can be continuously and relatively easy controlled by substitution. This paper presents the results of the magnetic behaviour of $MnCr_{2-2x}In_{2x}S_4$ crystals in the asymptotic critical temperature range as well as above this range for the substitution concentration region where long-range magnetic order exists.

§ Corresponding author.

0953-8984/99/407907+14$30.00

2. Experimental details

Polycrystalline $MnCr_{2-2x}In_{2x}S_4$ samples were prepared by the conventional solid state reaction method. Details of sample preparation and composition control were presented in [3]. Magnetic properties of the samples have been studied with the help of the vibrating sample magnetometer PAR 4500 in the 4.2–150 K temperature range and magnetic fields up to 1.6 T. The temperature was controlled by a PID Lake Shore 330 autotuning temperature controller which permits us to achieve stability better than 20 mK, which is important for critical region studies. Critical exponents were determined by commonly used techniques, i.e. modified Arrott plots, the Kouvel and Fisher method, ln M versus ln H_{eff} and scaling analysis, justified in detail in [6]. The effective field H_{eff} was calculated by subtracting the demagnetizing field from the applied field. The demagnetizing factor was obtained from low field ($\leqslant$10–50 Oe) magnetization measurements.

3. Experimental results

The magnetic isotherms in the region of phase transition for $MnCr_{2-2x}In_{2x}S_4$ samples with the In concentration in the range $0 \leqslant x \leqslant 0.10$ are typical for soft magnets and do not have any peculiarities. The low field temperature dependences of magnetization for these samples are characterized by a well pronounced kink, which is identified as a point of phase transition. With the increase of In concentration this kink becomes less sharp and shifts to lower temperatures, indicating the decrease of the temperature of the magnetic phase transition and the increase of disorder in the magnetic system (see figure 1 in [3]).

In figure 1(a)–(d) the modified Arrott plots obtained for different temperatures including the phase transition region are shown for four samples with various substitution concentrations. The plots are drawn using the 3D Heisenberg values of the critical exponents β and γ. Choice of these values was based on the data of fitting of the experimental curves passing through the origin (critical isotherms) by an expression [7]

$$(H_{eff}/M)^{1/\gamma} = k_1 t + k_2 M^{1/\beta} \tag{1}$$

which gives the value of the relation $\gamma/\beta = 3.80$–3.82 that is close to the Heisenberg one (here $t = |(T/T_C - 1)|$). A rather good linearity of the high field part of the dependences in a temperature range close to T_C was found for samples with low substitution concentration ($x \leqslant 0.05$). For strongly diluted samples ($x \geqslant 0.07$) an increase of the slope of the Arrott plot in the vicinity of T_C was observed as compared with low substitution ones.

The values of the saturation magnetization M_s and the inverse initial susceptibility χ_0^{-1} of the crystals have been correspondingly determined from these plots by the linear extrapolation from the high fields to the interception with $M^{1/\beta}$ and $(H_{eff}/M)^{1/\gamma}$ axes. Figures 2 and 3 present the temperature dependences of these parameters for the studied temperature range. The measurements in the vicinity of the transition temperature for $t < 5\times10^{-2}$ were performed with 0.1–0.15 K temperature steps and M_s data for this range are also shown in figure 2 by the open symbols. The exponents β and γ have been calculated by a single-power-law (SPL) analysis based on the approximation of the experimental data in the vicinity of the transition temperature by the expressions

$$M_s = m_0 t^{\beta} \tag{2}$$

and

$$\chi_0 = (m_0/h_0)t^{-\gamma} \tag{3}$$

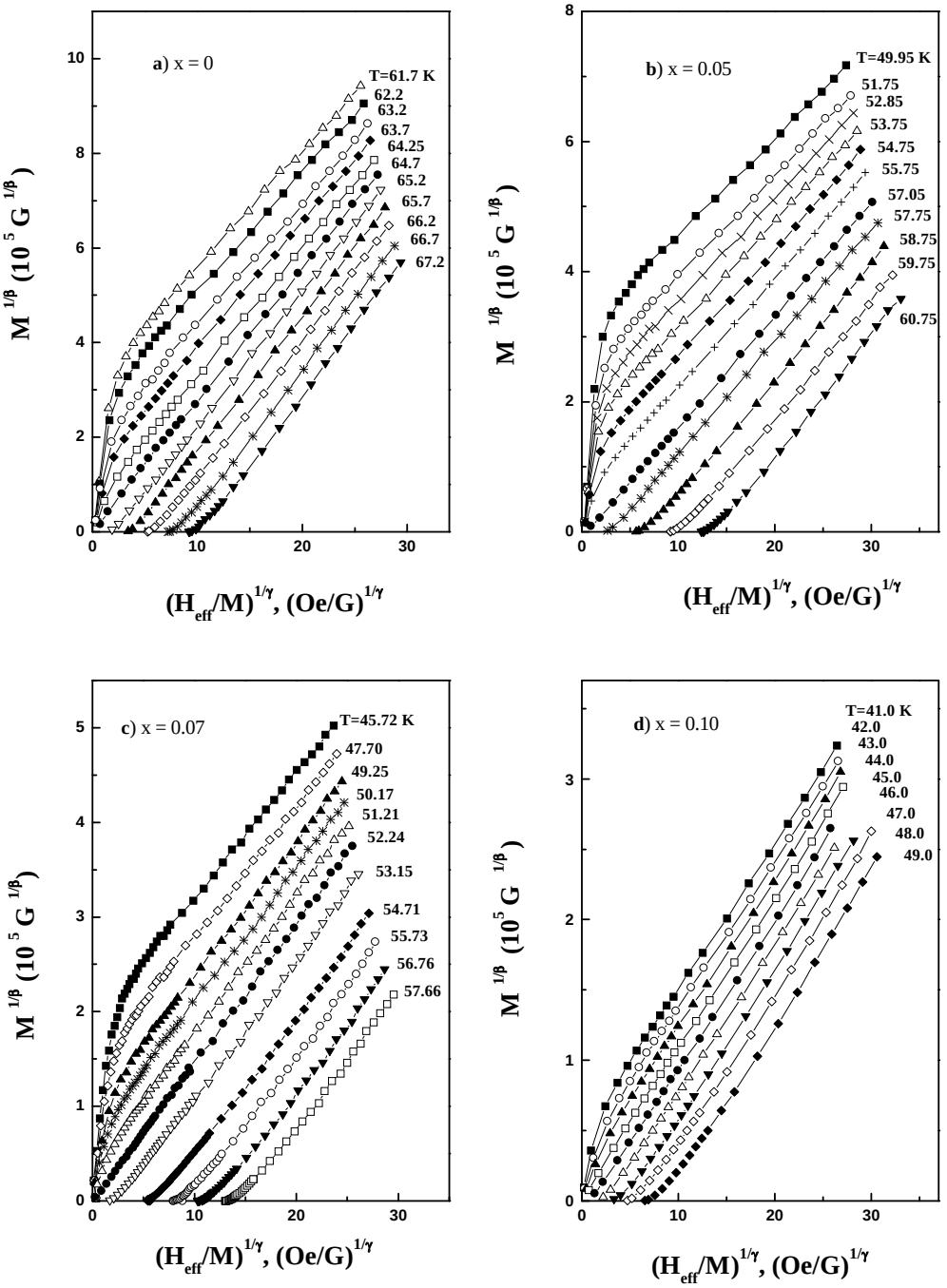

Figure 1. The modified Arrott plots for $MnCr_{2-2x}In_{2x}S_4$ crystals with different substitution concentration of In for Cr. The lines are only guides to the eye.

where m_0 and m_0/h_0 are the corresponding critical amplitudes. The fitting was done for various widths of the temperature range, selected to reach the lowest t value and to obtain the asymptotic values of critical parameters.

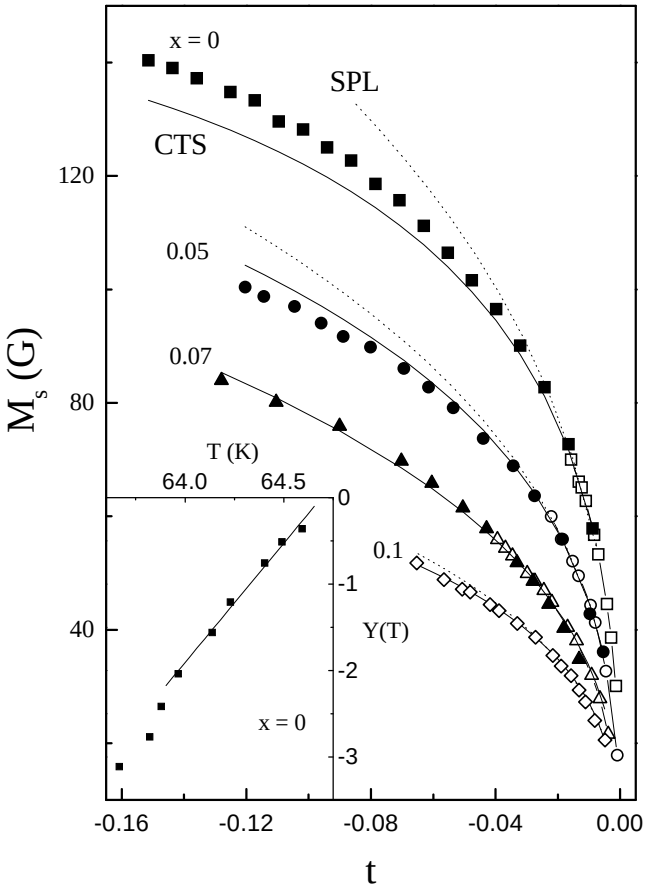

Figure 2. Saturation magnetization M_s against reduced temperature $t = (T - T_C)/T_C$ for various $MnCr_{2-2x}In_{2x}S_4$ samples.

The values of β and γ were also determined by the Kouvel–Fisher method [8] from the inverse slope of the functions

$$Y(T) = M_s^{-1}/(\mathrm{d}M_s^{-1}/\mathrm{d}T) \tag{4}$$

and

$$X(T) = \chi_0^{-1}/(\mathrm{d}\chi_0^{-1}/\mathrm{d}T) \tag{5}$$

in the asymptotic region. The $Y(T)$ and $X(T)$ temperature dependences for the sample with $x = 0$ are shown in the insets of figure 2 and 3.

In figure 4 the dependences of magnetization on the effective magnetic field H_{eff} on double logarithmic axes are presented for non-substituted $MnCr_4S_4$ sample in the vicinity of the Curie temperature. The isotherms exhibit a positive curvature for $T < T_C$ and a negative one for $T > T_C$. Similar dependences were observed for all the substituted samples and as was pointed out in [9] indicate the small magnetic anisotropy. The values of the third critical exponent δ and the critical amplitude D defined by the relation

$$H_{eff} = DM^{\delta} \tag{6}$$

were calculated by a linear regression of the critical isotherm.

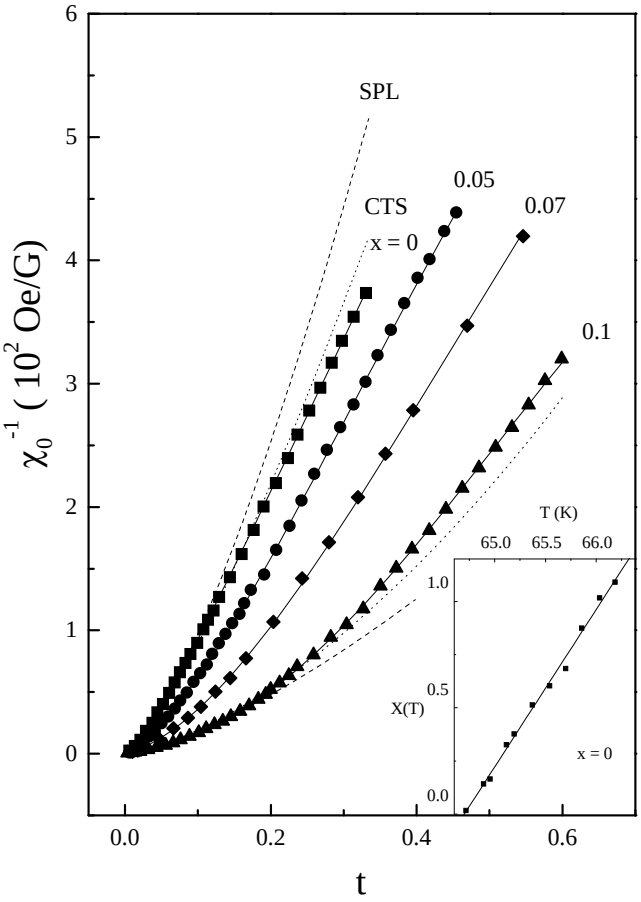

Figure 3. Inverse initial susceptibility χ_0^{-1} against reduced temperature t for studied crystals.

The critical parameters obtained by these different independent methods are listed in tables 1 and 2.

4. Discussion

4.1. Asymptotic region

The results of our detailed analysis of the critical phenomena in $MnCr_{2-2x}In_{2x}S_4$ crystals show that the values of the critical exponents determined by different methods are close to each other and to those of 3D Heisenberg model ($\gamma = 1.386$, $\beta = 0.3645$, $\delta = 4.8$ [10]). It is also found that structural disorder induced by magnetic dilution has a relatively small influence on the critical exponents. The tendency of a slight increase of the γ values for In rich samples may be considered a consequence of the decrease of critical region width with disorder increase as well as of the increase of slope of the Arrott plot, as indicated in [11].

It is well known that the values of the critical exponents obtained by KF and SPL analyses depend on the range of fit and are effective ones due to the averaging over the some temperature range. In order to obtain the correct values of the critical exponents the correction-to-scaling

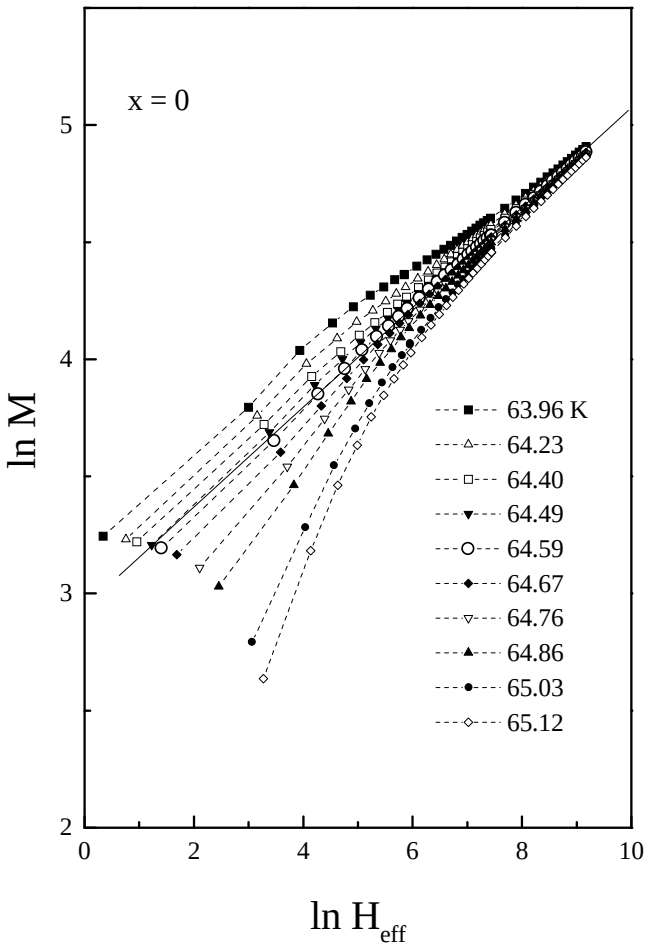

Figure 4. ln M–ln H_{eff} isotherms in the vicinity of the Curie temperature for the $MnCr_4S_4$ crystal (M in G, H_{eff} in Oe). The straight line through the data represents the least-squares fit to the critical isotherm. The dashed lines are only guides to the eye.

(CTS) terms [12–15] should be taken into consideration. The fitting to the experimental data was performed with the expressions including nonanalytical correction-to-scaling terms:

$$M_s = m_0 t^{\beta}[1 + a_M^- t^{\Delta}] \tag{7}$$

and

$$\chi_0 = (m_0/h_0)t^{-\gamma}[1 + a_\chi^+ t^{\Delta}] \tag{8}$$

keeping the value of $\Delta = 0.55$ predicted for 3D Heisenberg systems [16]. The results of this CTS analysis are also presented in table 1. CTS calculations slightly changed the exponent value in the indicated temperature range in comparison with SPL analysis both for pure ($x = 0$) and for substituted samples. However, the variation of the exponents has been within the calculation errors. Nonetheless, CTS fits describe the experimental data better than SPL fits in an extended temperature range (see figures 2 and 3). A comparison of the difference between SPL and CTS fits and the experimental data is illustrated by figures 5 and 6 for M_s and χ_0^{-1} respectively. From these plots the superiority of the CTS to SPL fits could be revealed in

Table 1. Some critical parameters of $MnCr_{2-2x}In_{2x}S_4$ crystals.

Substitution (x)	Analysis	Fit range t t (10^{-2})	T_C^- (K)	β	m_0 (G)	a_M^-
0	KF	1.1	64.69(1)	0.363(8)	320(6)	
	SPL	1.1	64.69(1)	0.367(9)	327(8)	
	SPL	1.6	64.70(1)	0.365(5)	320(8)	
	CTS	1.5	64.67(1)	0.369(4)	350(7)	−0.67(13)
0.05	KF	1.9	56.91(1)	0.372(4)	245(5)	
	SPL	1.0	56.90(1)	0.372(6)	250(20)	
	SPL	1.9	56.90(1)	0.363(4)	238(9)	
	CTS	1.9	56.87(1)	0.366(4)	250(9)	−0.33(13)
0.07	KF	2.5	52.25(1)	0.366(7)	180(18)	
	SPL	2.5	52.24(5)	0.360(16)	179(9)	
	SPL	3.8	52.26(3)	0.365(7)	181(4)	
	CTS	3.0	52.23(6)	0.365(12)	189(2)	−0.27(16)
0.10	KF	2.7	44.28(2)	0.369(18)	146(15)	
	SPL	2.7	44.26(5)	0.366(6)	141(5)	
	SPL	4.7	44.30(4)	0.361(4)	140(10)	
	CTS	4.7	44.23(3)	0.364(3)	154(3)	−0.42(7)
Substitution (x)	Analysis	Fit range t t (10^{-2})	T_C^+ (K)	γ	h_0/m_0 (Oe G^{-1})	a_χ^+
0	KF	1.6	64.66(1)	1.373(14)	2270(70)	
	SPL	1.6	64.65(1)	1.384(8)	2350(100)	
	CTS	1.6	64.66(1)	1.386(8)	2535(85)	0.59(26)
0.05	KF	1.8	56.85(1)	1.405(14)	1670(160)	
	SPL	1.8	56.86(1)	1.389(10)	1560(65)	
	CTS	1.8	56.86(1)	1.380(10)	1600(135)	0.5(6)
0.07	KF	2.6	52.21(1)	1.394(14)	755(75)	
	SPL	2.6	52.20(1)	1.387(14)	750(50)	
	CTS	2.6	52.20(1)	1.399(8)	720(80)	−0.7(3)
0.10	KF	2.8	44.32(2)	1.406(14)	470(60)	
	SPL	4.6	44.32(2)	1.391(18)	450(60)	
	CTS	4.6	44.31(2)	1.398(22)	430(50)	−0.4(1.3)

Table 2. Some critical parameters of $MnCr_{2-2x}In_{2x}S_4$ crystals.

Sub. (x)	γ/β (equation (1))	δ (equation (6))	D (10^{-6}) (Oe $G^{-\delta}$)	T_C (K) (equation (6))	γ (equation (10))	β (equation (10))	T_C (K) (equation (10))
0	3.813(8)	4.813(10)	0.58(2)	64.59(10)	1.37(1)	0.36(1)	64.7(1)
0.05	3.814(8)	4.814(10)	1.21(3)	56.79(10)	1.39(1)	0.36(1)	57.0(1)
0.07	3.813(8)	4.812(10)	1.63(4)	52.09(10)	1.38(1)	0.36(1)	52.1(1)
0.10	3.796(8)	4.795(10)	2.40(6)	44.06(15)	1.39(1)	0.36(1)	44.3(1)

the temperature range $|t| > 2 \times 10^{-2}$ for M_s and $|t| > 5 \times 10^{-2}$ for χ_0^{-1}. This difference was not so clear and it was difficult to give the priority to any of the fits for the narrower temperature range in the vicinity of T_C. We note here that even as small a $\Delta T = 0.1$ K step of the temperature change in the critical region is probably insufficient to obtain the better accuracy, because of the relatively high value of $\Delta T/T_C$. Furthermore, this relation increases with the substitution and contributes to the larger calculation errors for strongly disordered samples. Nevertheless, taking into account all the above mentioned considerations one can

conclude that the temperature range $|t| < 5 \times 10^{-2}$ lies within the asymptotic critical region and the determined values of the exponents present the correct critical rather then effective data. An additional point to emphasize is that calculated values of exponents, particularly those obtained from the fittings according to equation (1) and (6), satisfy well the Widom scaling relation [17]

$$\gamma = \beta(\delta - 1) \tag{9}$$

as indicated in table 2. It is also well known that the relation (9) assumes the data in the critical region to obey the scaling equation of state

$$m = f_{\pm}(h) \tag{10}$$

that describes two universal curves for $T < T_C$ and $T > T_C$. Here $m = M/t^{\beta}$ and $h = H_{eff}/t^{\beta+\gamma}$ are the scaled magnetization and the scaled field respectively. In figures 7(a)–(d) the scaling plots $\ln(M/t^{\beta}) = f\{\ln(H_{eff}/t^{\beta+\gamma})\}$ for studied crystals are shown. The collapse of these dependences on two branches for $T < T_C$ and for $T > T_C$ with the relatively small scattering of the data have been obtained for all the samples with the appropriate choice of variables β and γ and T_C. Their values are also presented in table 2 and are consistent with those calculated by the other methods. This confirms the complementary Heisenberg-like values of the asymptotic critical exponents in the $MnCr_{2-2x}In_{2x}S_4$ system.

It is necessary to point out here that the pure $MnCr_4S_4$ crystal is a good 3d Heisenberg magnet, taking into account the obtained asymptotic critical exponents. Using the well known relation between critical exponents β, γ and critical specific heat exponent $\alpha = 2(1 - \beta) - \gamma$ one can obtain that $\alpha = -0.12(3)$ for this crystal ($x = 0$). For this case the Harris criterion [18] predicts that chemical disorder should have no effect on the critical exponents. So, the observed behaviour of the critical exponents for disordered samples indicates that the Harris criterion is fulfilled for our system.

It should be also mentioned that a similar behaviour of critical parameters has been observed earlier in disordered crystalline Heisenberg ferro- and ferrimagnets, for example $Zn_xNi_{1-x}Fe_2O_4$ ferrites with spinel structure. For these materials no influence of disorder on the values of the asymptotic critical exponents was shown [19, 20]. On the other hand, spinel systems containing only one magnetic ion, for example $Cd_{1-x}Zn_xCr_2S_4$ or $Cd_{1-x}Zn_xCr_2Se_4$ show strong deviations from the Heisenberg values of the critical exponents [5]. Furthermore, for the similar $CdCr_{2-2x}In_{2x}S_4$ system the increase of the value of the critical exponent γ up to 1.97 for $x = 0.05$ has been reported [21]. Results obtained in this paper for the ternary magnetic $MnCr_{2-2x}In_{2x}S_4$ spinels together with mentioned results for similar systems could be explained phenomenologically in a following way. The performed experiments indicate clearly that the chemical disorder has no effect on the critical exponents for spinel systems consisting of two magnetic subsystems with one nearly completely chemically and magnetically ordered. It seems that the ordered subsystem suppresses the random fields in the disordered subsystem quenching in this way the disorder effects. An opposite effect probably exists in the systems with only one magnetic subsystem: $Cd_{1-x}Zn_xCr_2S_4$, $Cd_{1-x}Zn_xCr_2Se_4$ [5] or $CdCr_{2-2x}In_{2x}S_4$ [21]. In this case chemical disorder induces magnetic disorder in the magnetic subsystem through the random anisotropy or through the random changing of superexchange between magnetic ions. It should not be excluded also that systems with one magnetic sublattice are not good Heisenberg ones.

Table 3 presents some universal asymptotic amplitude ratios for studied crystals calculated using parameters given in table 1, experimentally determined magnetization data and theoretically predicted values by the Heisenberg model. From these data it may appear that only the Dm_0^{δ}/h_0 universal amplitude ratio is close to the theoretical value, whereas other quantities substantially differ from the predicted ones. The increased values of $m_0/M_s(0)$

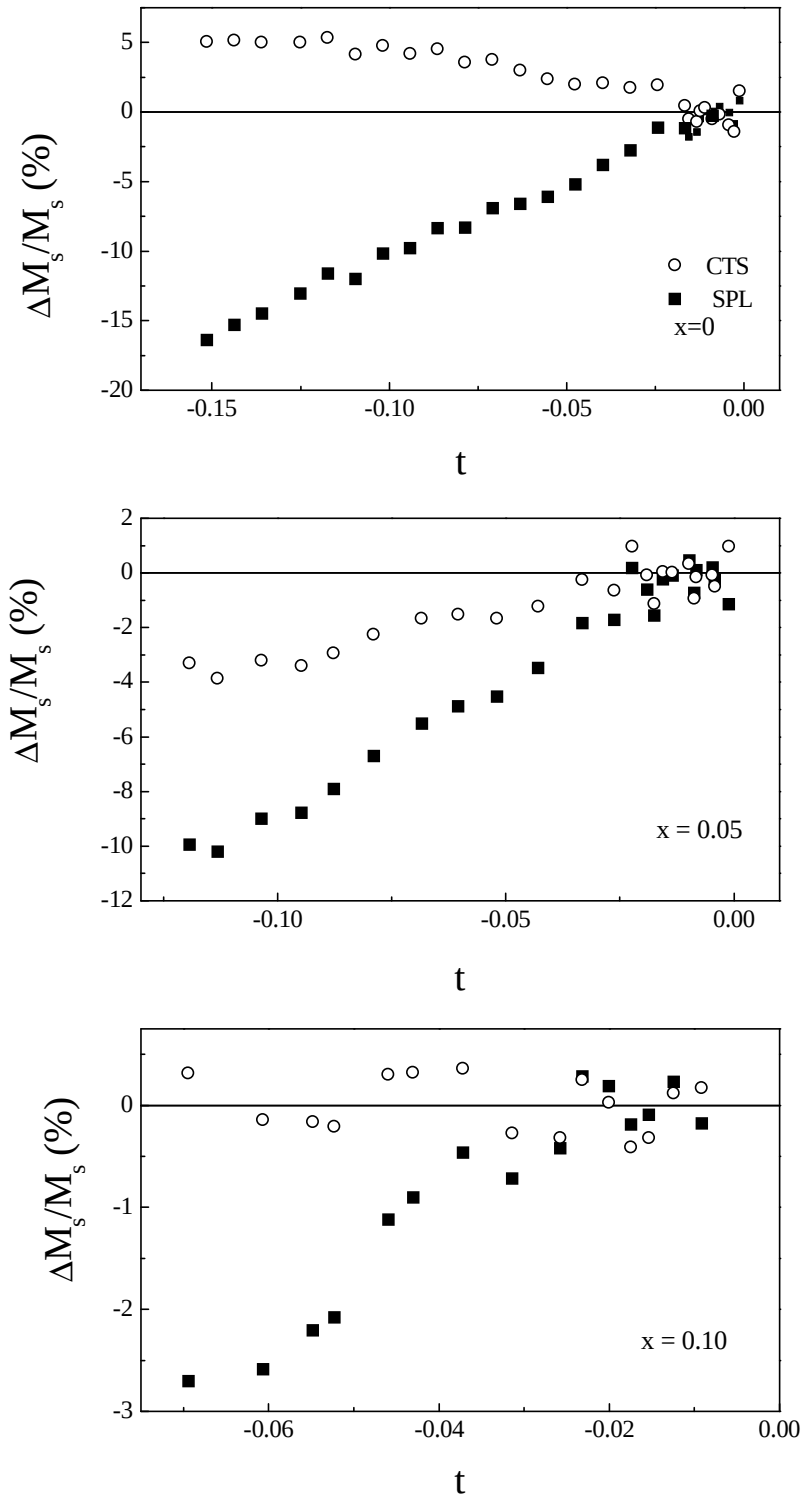

Figure 5. The relative deviation of the M_s values $(M_{exp} - M_{fit})/M_{exp}$, calculated by the SPL and CTS fits from the experimental data.

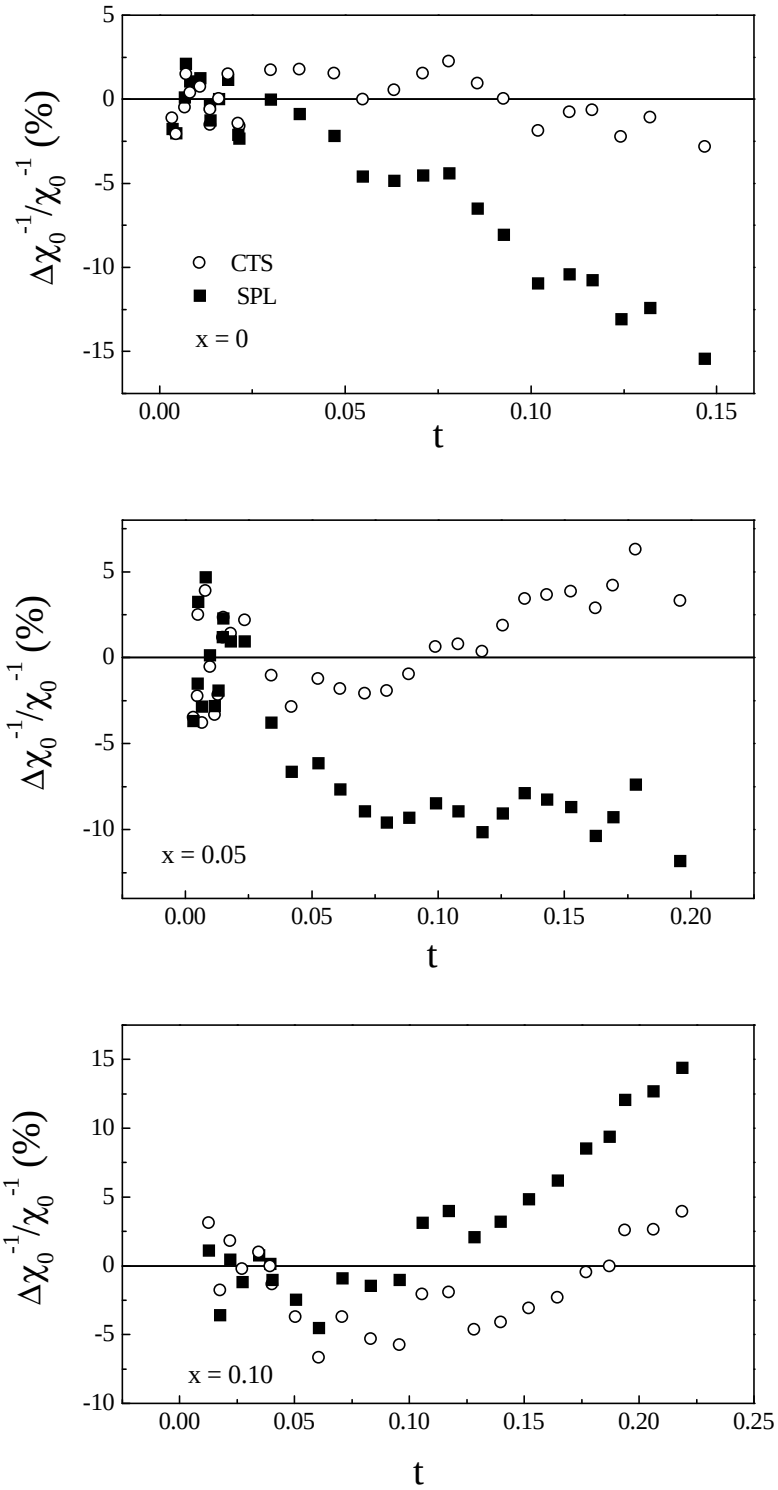

Figure 6. The relative deviation of the χ_0^{-1} values calculated by the SPL and CTS fits from the experimental data.

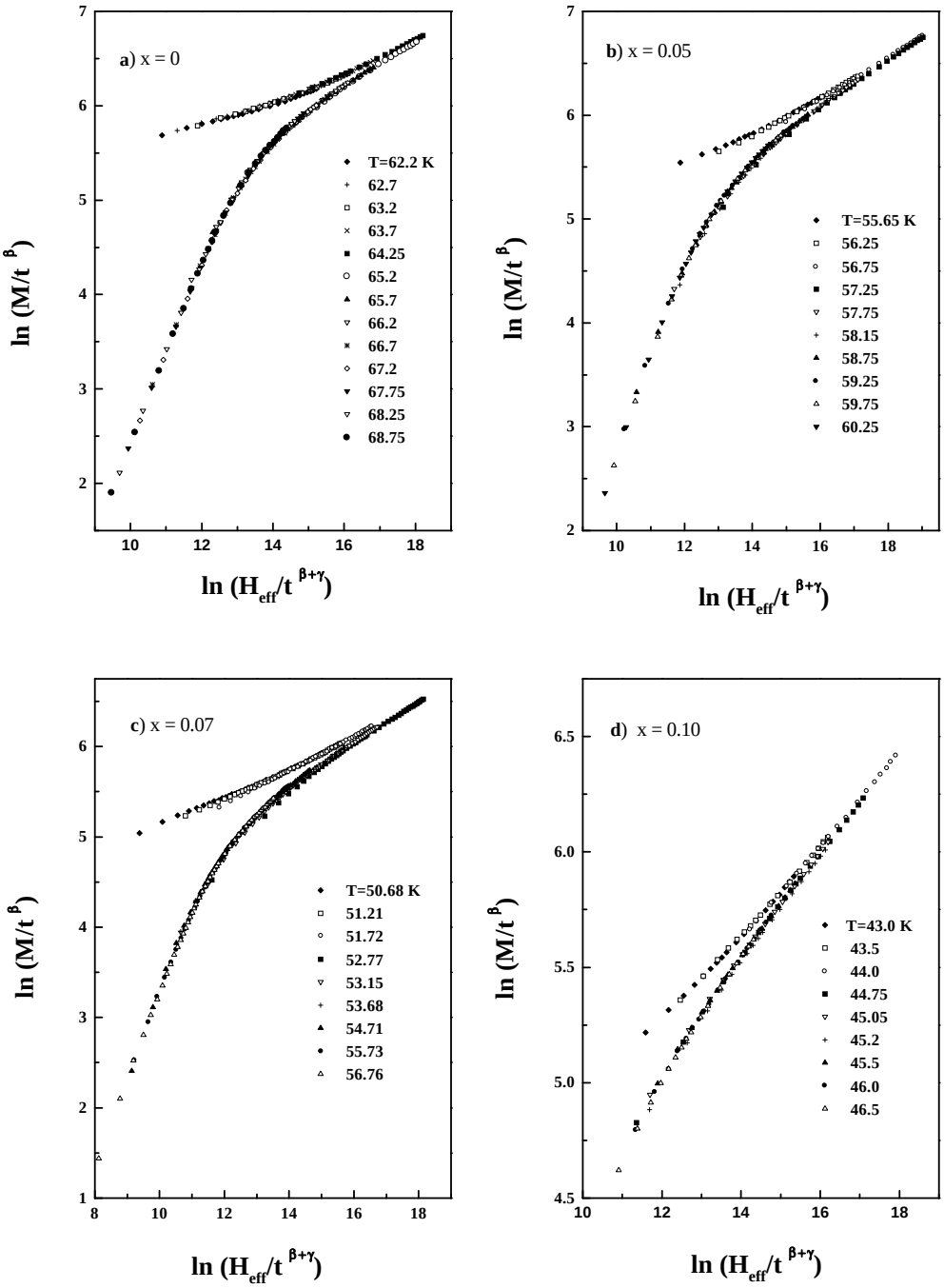

Figure 7. The scaling plots for different $MnCr_{2-2x}In_{2x}S_4$ crystals.

ratio probably result from the reduced magnetic moment due to ferrimagnetic alignment of Cr and Mn spins. However, very low values of the $\mu_0 h_0/k_B T_C$ ratio for the strongly disordered samples could not be explained in this way. This fact as pointed in [6] could testify that the

Table 3. Universal amplitude ratios for magnetization.

Substitution (x)	M_s (0) (G)	m_0/M_s (0)	μ_0 (μ_B)	$\mu_0 h_0/k_B T_C$	Dm_0^{δ}/h_0	μ_{eff} (μ_B)	c (%)
0	70(1)	5.0(4)	0.96(1)	0.88(9)	1.15(31)	1.7(1)	56(6)
0.05	85(1)	2.9(3)	1.20(1)	0.57(6)	1.06(40)	3.3(4)	36(4)
0.07	70(1)	2.7(3)	0.98(1)	0.20(2)	1.08(21)	9.0(1.0)	11(1)
0.10	46(2)	3.8(2)	0.67(3)	0.07(1)	1.12(35)	15.7(1.5)	4.3(5)
Theory [6]		1.37(7)		1.58	1.33 (1)		

number of spins participating in the ferrimagnetic to paramagnetic transition is substantially lower than expected by the 3D Heisenberg estimate μ_{eff}. Calculations made for our samples show that the concentration of these spins $c = \mu_0/\mu_{eff}$ decreases rapidly with the increase of disorder degree with the substitution.

4.2. High temperature region

The difference between ordered and disordered crystals in [19, 20] was found outside the critical region for the temperature dependences of the Kouvel–Fisher susceptibility exponent γ^* that is determined by the expression [8]

$$\gamma^* = (T - T_C)\chi_0(\mathrm{d}\chi_0^{-1}/\mathrm{d}T). \tag{11}$$

For calculating of the values of the inverse initial susceptibilities χ_0^{-1} outside the critical region we used the same linear extrapolation of modified Arrott plots as for the critical region. The χ_0^{-1} data obtained for the temperature range up to 0.4–0.6 T_C are also presented in figure 3. For the In-free sample ($x = 0$) the temperature region of the upward curvature of $\chi_0^{-1} = f(T)$ dependence was found to be rather low ($<0.05\ T_C$). With the increase of substitution concentration the considerable expansion of the temperature range of the upward curvature of $\chi_0^{-1} = f(T)$ has been observed. We have performed the fifth order polynomial fits as well as Pade approximants to the experimental data. Except the region close to T_C it was possible to obtain a good fit of χ_0^{-1} to the experimental data within 2–4% calculation errors. The full lines in figure 3 show these fits. From the fit data the values of γ^* have been calculated and the temperature dependences of γ^* for the studied samples are shown in figure 8. The non-monotonic temperature behaviour of γ^* having a maximum at the reduced temperature $t = 0.15$–0.3 is the general feature of these dependences for substituted samples. With the growth of the substitution concentration the increase of the γ^* values and shift of the γ^* maximum to higher temperatures were found. The maximum value of γ^* close to 1.8 obtained for samples with $x = 0.10$ may indicate the high disorder degree and is close to the value observed for strongly-disordered ZnNi ferrites [19, 20]. It should be also pointed out that concentration $x = 0.1$ is very close to the percolation threshold $x = 0.12$ for this system, as found recently [22], and correlates with the earlier results [3]. For $MnCr_4S_4$ sample the monotonic decrease of $\gamma^*(T)$ has been observed with temperature increase, except the small region close to T_C where $\gamma^*(T)$ changed non-monotonically indicating some disorder. It may result from the redistribution of a fraction of the Mn ions between A and B sites of the spinel lattice. However, this redistribution effect was established only for highly In-substituted samples [23]. It is noteworthy to mention that the spin-glass-like behaviour of magnetization at low temperatures that we observed in this sample [3] also indicates some degree of disorder.

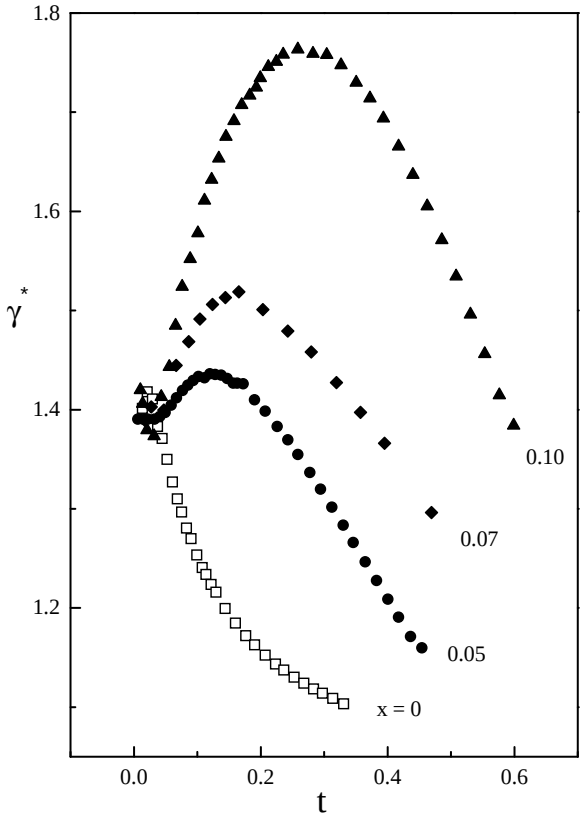

Figure 8. The Kouvel–Fisher susceptibility exponent γ^* against reduced temperature t for different $MnCr_{2-2x}In_{2x}S_4$ crystals.

5. Conclusions

The following main conclusions can be reached, based on the results of the present study.

The first is that critical exponents of the studied crystals of $MnCr_{2-2x}In_{2x}S_4$ systems determined by different independent methods are close to each other and are consistent with those predicted by the 3D Heisenberg model.

The second one is that chemical disorder induced by magnetic dilution of the Cr subsystem by In has low influence on the asymptotic values of the critical exponents. Thus, the Harris criterion is fulfilled for this system consisting of two magnetic ions. A scaling equation of state is obeyed for all the samples independent of the disorder degree. It has been also suggested that the presence of the Mn-subsystem strongly coupled with the chromium ions is responsible for this effect, while for similar spinel systems with one magnetic ion the chemical disorder could influence the magnetic subsystem through the random anisotropy or the random superexchange.

The third conclusion implies the different temperature behaviour of the Kouvel–Fisher susceptibility exponent γ^* outside the critical region: monotonic decrease of γ^* for pure and non-monotonic dependences of γ^* for disordered samples, as well as the increase of the maximum γ^* values with the disorder increase.

Finally, we want to underline that the behaviour of the critical exponents as well as of the Kouvel–Fisher susceptibility exponent γ^* is similar to those observed in many disordered

crystalline Heisenberg ferro- and ferrimagnets, and is consistent with the theoretical predictions for isotropic three-dimensional systems with short-range exchange interactions [24, 25].

Acknowledgment

We are very grateful to Professor S N Kaul for helpful discussions.

References

[1] Menyuk N, Dwight K and Wold A 1965 *J. Appl. Phys.* **36** 1088
[2] Darcy L, Baltzer P K and Lopatin E 1968 *J. Appl. Phys.* **39** 898
[3] Tsurkan V, Baran M, Szymczak R and Szymczak H 1997 *J. Magn. Magn. Mater.* **172** 317
[4] Dormann J L and Nogues M 1991 *Phase Transitions* **33** 159
[5] Belyachi A, Dormann J L and Nogues M 1998 *J. Phys.: Condens. Matter* **10** 1599
[6] Kaul S N 1985 *J. Magn. Magn. Mater.* **53** 5
[7] Arrott A and Noakes J E 1967 *Phys. Rev. Lett.* **19** 786
[8] Kouvel J S and Fisher M E 1964 *Phys. Rev.* A **136** 1626
[9] Reisser R, Seeger M and Kronmuller H 1993 *J. Magn. Magn. Mater.* **128** 321
[10] Le Guillou J C and Zinn-Justin J 1980 *Phys. Rev.* B **21** 3976
[11] Yeung I, Roshko R M and Williams G 1986 *Phys. Rev.* B **34** 3456
[12] Wegner F J 1972 *Phys. Rev.* B **5** 4529
[13] Aharony A and Ahlers G 1980 *Phys. Rev. Lett.* **44** 782
[14] Kaul S N 1994 *Phase Transitions* **47** 23
[15] Babu P D and Kaul S N 1997 *J. Phys.: Condens. Matter* **9** 7189
[16] Le Guillou J C and Zinn-Justin J 1977 *Phys. Rev. Lett.* **39** 95
[17] Widom B 1965 *J. Chem. Phys.* **43** 3892
[18] Harris A B 1974 *J. Phys. C: Solid State Phys.* **7** 1671
[19] Haug M, Fahnle M and Kronmuller H 1987 *J. Magn. Magn. Mater.* **69** 163
[20] Haug M, Fahnle M, Kronmuller H and Haberey F 1987 *Phys. Status Solidi* b **144** 411
[21] Pouget S, Alba M and Nogues M 1994 *J. Appl. Phys.* **75** 5826
[22] Tsurkan V 1998 *Balkan Phys. Lett.* **6** 227
[23] Lutz H D and Jung M 1989 *Z. Anorg. (Allg.) Chem.* **579** 57
[24] Fahnle M and Haug M 1987 *Phys. Status Solidi* b **140** 569
[25] Fahnle M 1987 *J. Magn. Magn. Mater.* **65** 1